



# Towards parametrising atmospheric concentrations of ice nucleating particles active at moderate supercooling

Claudia Mignani<sup>a</sup>, Jörg Wieder<sup>b</sup>, Michael A. Sprenger<sup>b</sup>, Zamin A. Kanji<sup>b</sup>, Jan Henneberger<sup>b</sup>, Christine Alewell<sup>a</sup>, and Franz Conen<sup>a</sup>

<sup>a</sup>Department of Environmental Sciences, University of Basel, Bernoullistrasse 30, 4056 Basel, Switzerland

<sup>b</sup>Institute for Atmospheric and Climate Science, ETH Zurich, Universitätsstrasse 16, 8092 Zurich, Switzerland

**Correspondence:** Claudia Mignani (claudia.mignani@unibas.ch) or Franz Conen (franz.conen@unibas.ch)

**Abstract.** A small fraction of freezing cloud droplets probably initiates much of the precipitation above continents. Only a minute fraction of aerosol particles, so-called ice nucleating particles (INPs), can trigger initial ice formation at  $-15\text{ °C}$ , a cloud-top temperature frequently associated with snowfall. We found at a mountain top site in the Swiss Alps that concentrations of INPs active at  $-15\text{ °C}$  are different functions of coarse ( $> 2\text{ }\mu\text{m}$ ) aerosol particle concentrations, depending on whether an air mass is precipitating, non-precipitating, or carrying Saharan dust and non-precipitating. Consequently, we suggest that a parameterisation at moderate supercooling should consider coarse particles in combination with air mass differentiation.

## 1 Introduction

Ice nucleating particles (INPs) affect clouds and their development by generating primary ice at temperatures between 0 and  $-38\text{ °C}$ . The difficulty of understanding and thus predicting atmospheric INP concentrations ([INP]) originates from the complex interplay of their rarity, their various sources, and nucleation temperatures (Paramonov et al., 2019). A current empirical parameterisation established by DeMott et al. (2015), hereafter D15, predicts [INP] based on nucleation temperature and number concentration of aerosol particles with diameters  $>0.5\text{ }\mu\text{m}$  ( $[n_{0.5}]$ ) (DeMott et al., 2015). Although successful at colder temperatures, it remains "weakly constrained at temperatures  $>-20\text{ °C}$ , where much additional ambient and laboratory data are needed" (DeMott et al., 2015). Parametrising [INP] in the warmer temperature range is important because cloud-top temperatures associated with winter precipitation have a distinct temperature mode near  $-15\text{ °C}$ , as derived from close to  $10^5$  parallel observations of cloud-top temperatures and falling solid precipitation throughout the United States (Hanna et al., 2008). The same mode may also occur in other continental regions in the midlatitudes as it makes physically sense for various reasons (Wetzel and Martin, 2001). Recent findings from size-resolved measurements of atmospheric INPs show that those active at  $-15\text{ °C}$  or warmer ( $\text{INPs}_{-15}$ ) are mostly  $>2.0\text{ }\mu\text{m}$  in diameter (Huffman et al., 2013; Mason et al., 2016; Creamean et al., 2015), a particle size that is poorly represented for instrumental reasons in the empirical data on which D15 and other parameterisations (Phillips et al., 2013) are based. A further finding is the increased atmospheric abundance of such INPs during precipitation



(Bigg and Miles, 1964; Huffman et al., 2013; Hara et al., 2016; Conen et al., 2017). To test whether these findings can be reconciled with the general approach of D15 (i.e. parametrising INPs as a function of particles larger than a certain size), we collected and analysed aerosol samples from February to March 2019 at Weissfluhjoch, Switzerland, at average local air temperatures of  $-7.1$  (s.d.  $\pm 4.3$ ) °C during sampling intervals. The site, surrounding mountains and nearby valleys were snow-covered, most of the lowland was not and it received precipitation as rain.

## 2 Material and Method

Between 11 February and 26 March 2019, we collected and analysed a total of 124 aerosol samples at Weissfluhjoch, Switzerland ( $46^{\circ}49'58.670''\text{N}$ ,  $9^{\circ}48'23.309''\text{E}$ , 2671.1 m a.s.l.) during the "Role of Aerosols and Clouds Enhanced by Topography on Snow (RACLETS)" campaign. Total aerosol was sampled through a heated inlet at a flow rate of  $300 \text{ L min}^{-1}$  for 20 min (i.e.  $6 \text{ m}^3$  of air each) into 15 mL of ultra-pure water (Sigma-Aldrich, W4502-1L) using a high flow-rate impinger (Bertin Technologies, Coriolis® $\mu$ ). Evaporative losses were compensated by replenishing the circulating water after 10 and 20 min. Samples were analysed immediately after collection in a drop freezing assay, with 52 droplets of 100  $\mu\text{L}$  each, as previously described (Stopelli et al., 2014) and cumulative [INP] were calculated (Vali, 1971). The detection range of [INP] lies between  $5 \times 10^{-4}$  and  $0.2 \text{ std L}^{-1}$ . Samples outside this range (15 above, 1 below range) were not considered. Background measurements ( $n = 15$ ) following identical procedure, but without turning on airflow, were below detection limit. Number concentrations of particles [n] were measured continuously with an Aerodynamic Particle Sizer (APS) spectrometer 3321 from TSI Corporation and were averaged over the time-period of the impinger samples.  $[n_{0.5}]$  and  $[n_{2.0}]$  are the sum of all counts of particles  $\geq 0.542 \mu\text{m}$  and  $\geq 1.982 \mu\text{m}$ , respectively. [n] and [INP] were adjusted to standard pressure conditions ( $P_{\text{ref}} = 1013.25 \text{ hPa}$ ). Five-day back trajectories were calculated using the Lagrangian analysis tool LAGRANTO (Sprenger and Wernli, 2015). For each sample, one trajectory was started at the full hour closest to the sampling time and from the exact sampling position. The driving wind fields are taken from the operational analysis of the Swiss National Weather Service (COSMO1; www.meteoswiss.ch) and the European Centre for Mid-Range Weather Forecasts (ECMWF; www.ecmwf.int). Started in the COSMO domain, the trajectories were extended based on ECMWF data at the time and location where they leave this domain. Their position was saved every 10 min. Along the trajectories, total precipitation was traced amongst others enabling us to determine the total precipitation amount along the last 6 hours prior to sampling.

## 3 Results and Discussion

From a total of 124 aerosol samples, about half (56) were collected from air masses that had precipitated at least 1.0 mm during the 6 hours prior to sampling (defined as "precipitating"). About half of these air masses were also precipitating when sampled at Weissfluhjoch, as observed by a precipitation gauge. A similar number of samples (57) were from air masses with less or without any prior precipitation ("non-precipitating") and 11 were from air masses carrying Saharan dust (SD) and no prior precipitation. Air masses were mainly reaching the sampling position from the West. Precipitating air masses were



coming on a rather direct way from the Atlantic crossing the West of Europe with less detour than non-precipitating air masses  
55 whereas air masses carrying dust where coming from the direction of the Saharan desert passing the South of Europe (Fig.  
1a-c). Precipitating air masses had the lowest  $[n_{0.5}]$  and the lowest concentration of aerosol particles with diameters  $>2.0 \mu\text{m}$   
( $[n_{2.0}]$ ), but similar ratios as non-precipitating air masses of  $[n_{2.0}]$  to  $[n_{0.5}]$  (Fig. 1d-f). The largest ratio of  $[n_{2.0}]$  to  $[n_{0.5}]$  was  
in SD air masses (Fig. 1f). Atmospheric concentrations of INPs<sub>15</sub> ( $[\text{INP}_{15}]$ ) in non-precipitating air masses were closest to  
the parametrisation of D15, based on  $[n_{0.5}]$ . Although the D15 parametrisation predicts the overall median  $[\text{INP}_{15}]$  reasonably  
60 well ( $0.005 \text{ std L}^{-1}$ , versus the measured  $0.016 \text{ std L}^{-1}$ ), 72% of measured data was within a factor of 10, but only 29% within a  
factor of 2 of the prediction. Specifically, the D15 parametrisation tends to underestimate the median  $[\text{INP}_{15}]$  in precipitating  
air masses by roughly one order of magnitude and overestimates those in SD air masses by about the same factor (Fig. 1g).  
Considering the fact that the observed size of INPs<sub>15</sub> is mostly larger than  $2 \mu\text{m}$  (Huffman et al., 2013; Mason et al., 2016;  
Creamean et al., 2015), we plot measured  $[\text{INPs}_{15}]$  against  $[n_{2.0}]$ , instead of  $[n_{0.5}]$ , resulting in a more distinct separation  
65 of the data to the different air masses (Fig. 1h). The greater clarity of the separation confirms that  $[n_{2.0}]$  is a more powerful  
predictor of INPs<sub>15</sub> when combined with air mass differentiation. The clearer separation goes hand in hand with the earlier  
observation that air masses influenced by SD carry less INPs active at moderate supercooling per unit mass of aerosol particles  
than European background air masses (Conen et al., 2015). It also reveals the known enrichment of the aerosol population with  
highly efficient INPs during precipitation (Bigg and Miles, 1964; Huffman et al., 2013). In each of the three categories of air  
70 mass  $[\text{INP}_{15}]$  can be described as a function of  $[n_{2.0}]$  that is valid for a range of  $[\text{INP}_{15}]$  from  $0.0005 \text{ std L}^{-1}$  to  $0.2 \text{ std L}^{-1}$  (Fig.  
1h). The functions for data in SD and non-precipitating air masses appear to have similar slopes on a log-log plot. A possible  
explanation of additional INPs in precipitating air masses is the aerosolisation of INPs by rain itself, a mechanism that could  
be similar to the generation of bioaerosol by raindrop impingement (Joung et al., 2017). Since aerosolisation of efficient INPs  
during precipitation is likely independent of the background in  $[\text{INP}]$ , we may describe  $[\text{INP}_{15}]$  in precipitating air masses by  
75 adding a constant to the function fitted to the non-precipitating cases (Fig. 1h). The median difference between this function  
and measured  $[\text{INP}_{15}]$  in precipitating air masses was  $0.014 \text{ std L}^{-1}$  (Fig. 1i). The relationship between these differences and  
 $[n_{2.0}]$  were weakly positive and not significant (Person correlation test,  $R = 0.0027$  and  $p = 0.98$ ), meaning that the absolute  
value of additional INPs during precipitation was independent of  $[n_{2.0}]$ . A consequence of this finding is that to air masses  
with low  $[n_{2.0}]$  and thus low  $[\text{INP}_{15}]$ , the addition of INPs aerosolised by precipitation makes a relatively large contribution  
80 to the overall  $[\text{INP}_{15}]$ . The additional INPs during precipitation could be fungal spores emitted from the snow-free lowland of  
Switzerland and southern Germany, an explanation supported by observations of considerable presence of fungal spores in air  
during humid periods (Negron et al., 2020).

#### 4 Conclusions

In summary, it is possible to reconcile two fundamental aspects of INPs active at moderate supercooling - increased abundance  
85 during precipitation and size - with a widely used approach to parametrise INPs active at colder temperatures. Our study is  
the first to demonstrate the potential of differentiating between air masses that are precipitating, non-precipitating, or carrying



desert dust to predict INP concentrations. Future observations need to constrain the presented parametrisation functions in a wider geographical context. Particular attention has to be attributed to sampling at mixed-phase cloud height and including larger aerosol particles, as was done in this study. The more differentiated parameterisation including air mass history is a promising way towards predicting INPs active at around  $-15$  °C, which probably trigger much of the precipitation above midlatitude continental regions during winter.

## 5 Data availability

<https://www.envidat.ch/group/about/raclets-field-campaign>

*Author contributions.* CM and FC conceived the study. CM and JW conducted the measurements. JW provided the aerosol data. MAS conducted the modeling. ZAK and JH hosted the entire measurement campaign. CM and FC interpreted the data and wrote the manuscript with contributions from JW, MAS, ZAK, JH and CA.

*Competing interests.* The authors declare no competing interest.

*Acknowledgements.* We are indebted to Martin Genter for logistical support, Carolin Rösch and Michael Rösch for technical support, Nora Els for borrowing the Coriolis@ $\mu$  of University of Innsbruck as well as sharing her experience and Lucie Roth and Mario Schär for helping with the measurements. We thank MeteoSwiss for weather data and providing access to the COSMO1 and ECMWF data and all the RACLETS members for fruitful discussions. JH, JW and ZAK as well as CM and FC acknowledge funding from the Swiss National Science Foundation (SNSF) grant numbers 200021\_175824 and 200021\_169620, respectively.



## References

- Bigg, E. K. and Miles, G. T.: The results of large-scale measurements of natural ice nuclei, *J. Atmos. Sci.*, 21, 396–403, 1964.
- 105 Conen, F., Rodríguez, S., Hüglin, C., Henne, S., Herrmann, E., Bukowiecki, N., and Alewell, C.: Atmospheric ice nuclei at the high-altitude observatory Jungfraujoch, Switzerland, *Tellus B*, 67, 2015.
- Conen, F., Eckhardt, S., Gundersen, H., Stohl, A., and Yttri, K. E.: Rainfall drives atmospheric ice-nucleating particles in the coastal climate of southern Norway, *Atmos. Chem. Phys.*, 17, 11 065–11 073, 2017.
- Creamean, J. M., Ault, A. P., White, A. B., Neiman, P. J., Ralph, F. M., Minnis, P., and Prather, K. A.: Impact of interannual variations  
110 in sources of insoluble aerosol species on orographic precipitation over California’s central Sierra Nevada, *Atmos. Chem. Phys.*, 15, 6535–6548, 2015.
- DeMott, P. J., Prenni, A. J., McMeeking, G. R., Sullivan, R. C., Petters, M. D., Tobo, Y., Niemand, M., Möhler, O., Snider, J. R., Wang, Z., and Kreidenweis, S. M.: Integrating laboratory and field data to quantify the immersion freezing ice nucleation activity of mineral dust particles, *Atmos. Chem. Phys.*, 15, 393–409, 2015.
- 115 Hanna, J. W., Schultz, D. M., and Irving, A. R.: Cloud-top temperatures for precipitating winter clouds, *J. Appl. Meteorol. Climatol.*, 47, 351–359, 2008.
- Hara, K., Maki, T., Kobayashi, F., Kakikawa, M., Wada, M., and Matsuki, A.: Variations of ice nuclei concentration induced by rain and snowfall within a local forested site in Japan, *Atmos. Environ.*, 127, 1–5, 2016.
- Huffman, J. A., Prenni, A. J., DeMott, P. J., Pöhlker, C., Mason, R. H., Robinson, N. H., Fröhlich-Nowoisky, J., Tobo, Y., Després, V. R.,  
120 Garcia, E., Gochis, D. J., Harris, E., Müller-Germann, I., Ruzene, C., Schmer, B., Sinha, B., Day, D. A., Andreae, M. O., Jimenez, J. L., Gallagher, M., Kreidenweis, S. M., Bertram, A. K., and Pöschl, U.: High concentrations of biological aerosol particles and ice nuclei during and after rain, *Atmos. Chem. Phys.*, 13, 6151–6164, 2013.
- Joung, Y. S., Ge, Z., and Buie, C. R.: Bioaerosol generation by raindrops on soil, *Nat. Commun.*, 8, 2017.
- Mason, R. H., Si, M., Chou, C., Irish, V. E., Dickie, R., Elizondo, P., Wong, R., Brintnell, M., Elsasser, M., Lassar, W. M., Pierce, K. M.,  
125 Leaitch, W. R., MacDonald, A. M., Platt, A., Toom-Sauntry, D., Sarda-Estève, R., Schiller, C. L., Suski, K. J., Hill, T. C. J., Abbatt, J. P. D., Huffman, J. A., DeMott, P. J., and Bertram, A. K.: Size-resolved measurements of ice-nucleating particles at six locations in North America and one in Europe, *Atmos. Chem. Phys.*, 16, 1637–1651, 2016.
- Negron, A., DeLeon-Rodriguez, N., Waters, S. M., Ziemba, L. D., Anderson, B., Bergin, M., Konstantinidis, K. T., and Nenes, A.: Using flow cytometry and light-induced fluorescence to characterize the variability and characteristics of bioaerosols in springtime in Metro Atlanta,  
130 Georgia, *Atmos. Chem. Phys.*, 20, 1817–1838, 2020.
- Paramonov, M., Drossaert van Dusseldorp, S., Gute, E., Abbatt, J. P. D., Heikkilä, P., Keskinen, J., Chen, X., Luoma, K., Heikkinen, L., Hao, L., Petäjä, T., and Kanji, Z. A.: Condensation/immersion mode ice nucleating particles in a boreal environment, *Atmos. Chem. Phys. Discuss.*, 2019.
- Phillips, V. T. J., DeMott, P. J., Andronache, C., Pratt, K. A., Prather, K. A., Subramanian, R., and Twohy, C.: Improvements to an Empirical  
135 Parameterization of Heterogeneous Ice Nucleation and Its Comparison with Observations, *J. Atmos. Sci.*, 70, 378–409, 2013.
- Sprenger, M. and Wernli, H.: The LAGRANTO Lagrangian analysis tool – version 2.0, *Geosci. Model Dev.*, 8, 2569–2586, 2015.
- Stopelli, E., Conen, F., Zimmermann, L., Alewell, C., and Morris, C. E.: Freezing nucleation apparatus puts new slant on study of biological ice nucleators in precipitation, *Atmos. Meas. Tech.*, 7, 129–134, 2014.



- 140 Vali, G.: Quantitative evaluation of experimental results on the heterogeneous freezing nucleation of supercooled liquids, *J. Atmos. Sci.*, 28, 402–409, 1971.
- Wetzel, S. W. and Martin, J. E.: An operational ingredients-based methodology for forecasting midlatitude winter season precipitation, *Weather and Forecasting*, 16, 156–167, 2001.

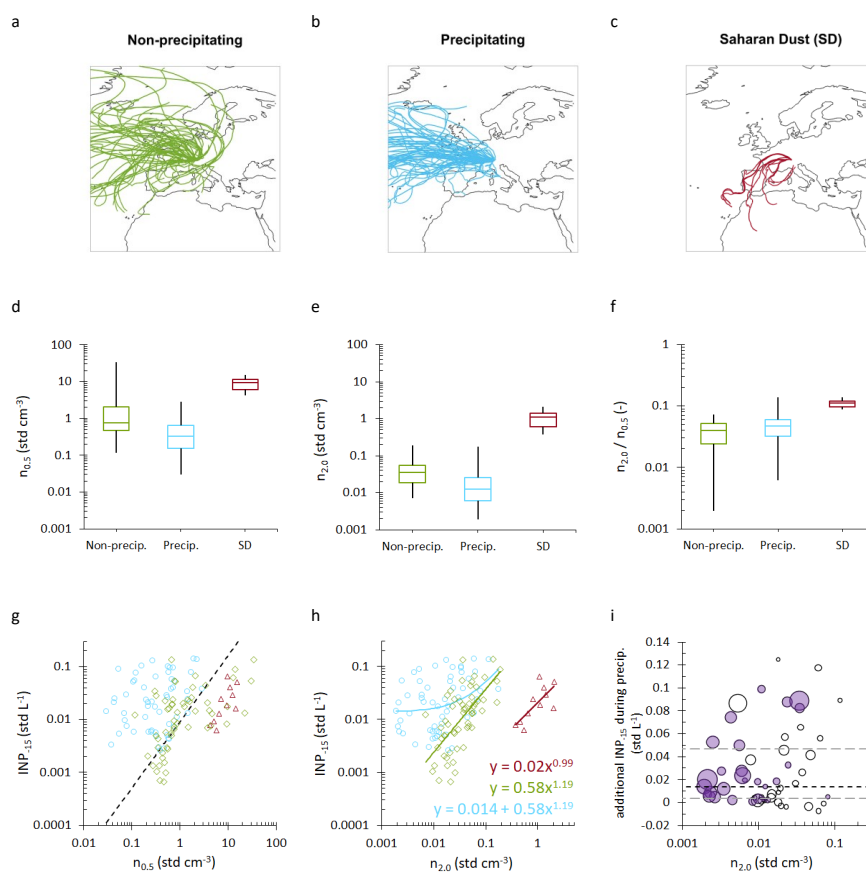


**Figure 1.** Separation of INP abundance in aerosol populations of air masses that were non-precipitating (green), precipitating (blue), and carrying Saharan Dust (SD, red). (a, b, c) Backward trajectories of air masses. Number concentrations of aerosol particles with diameters (d)  $>0.5 \mu\text{m}$  [ $n_{0.5}$ ] and (e)  $>2.0 \mu\text{m}$  [ $n_{2.0}$ ] and (f) their ratio. Concentrations of ice nucleating particles active at  $-15^\circ\text{C}$  or warmer [ $\text{INP}_{-15}$ ] (g) versus [ $n_{0.5}$ ] and (h) versus [ $n_{2.0}$ ] for precipitating (circles), non-precipitating (diamonds) and SD air masses (triangles). The D15 parametrisation extrapolated to  $-15^\circ\text{C}$  is shown as a black, dashed line. Preliminary parametrisations based on [ $n_{2.0}$ ] for non-precipitating and SD air masses are power functions. The function for precipitating air masses is the same as for non-precipitating air masses but with an added constant equivalent to  $0.014 \text{ INPs L}^{-1}$ . (i) Difference between [ $\text{INP}_{-15}$ ] in precipitating air masses and the function fitted to the non-precipitating air masses. The median difference is  $0.014 \text{ std L}^{-1}$  (black line) and the lower and upper quartiles are  $0.003$  and  $0.047 \text{ std L}^{-1}$ , respectively (grey lines). Circle area is proportional to the amount of precipitation along the last 6 hours of the trajectory prior to sampling. Filled symbols are for samples precipitating at Weissfluhjoch.